



Variation of organics, nitrogen and phosphorus within a cycle of a Bio-Denipho system

Jinming Duan^{a,*}, Wei Li^a, Kai Zhao^b, Joerg Krampe^c

^aKey Laboratory of Northwest Water Resource, Environment and Ecology, MOE, Xi'an University of Architecture and Technology, Xi'an 710055 China

Tel. +86 29 82201354; emails: jinmingduan@xauat.edu.cn, jinmingduan@hotmail.com

^bBeishiqiao Wastewater Treatment Corporation, Xi'an, China

^cSA Water Corporation, 250 Victoria Square, Adelaide SA 5000

Received 28 September 2010; Accepted 2 November 2011

ABSTRACT

Profiles of chemical oxygen demand (COD), dissolved oxygen (DO), ammonia nitrogen (NH_4^+-N), nitrate nitrogen (NO_x-N) and phosphorus (P) were established in a cycle of a four-phased Bio-Denipho process. Based on a unit-flow model and the ASM2d, organics degradation, nitrification and denitrification, and phosphorus removal processes were analysed. A switch function has been introduced to address the difference in DO concentrations between the core of biomass flocs and their outer-layers or the bulk suspensions. The calculations indicate that approximately 68% of the denitrification and nitrogen removal resulted from reactions within the anoxic cores of the biomass flocs, where DO was around 0.1 mg l^{-1} or less. This proved to be important mechanisms to phosphorus removal in the model for the four phased ditches. The analyses provide an insight in the nitrification, denitrification, and phosphorus removal mechanisms in such operation system, which is useful for the system diagnosis and optimisation.

Keywords: Activated sludge; Phased isolation ditch; ASM2d model; Bio-Denipho; Nitrification; Denitrification; Phosphorus removal

1. Introduction

Nutrient contamination of natural water resources from wastewater effluent disposal is an increasingly problematic issue [1]. Tight regulation of effluent nutrient concentrations requires high efficiency nitrogen (N) and phosphorus (P) removal. N removal is achieved via nitrification and denitrification processes. Conventionally these two processes can be either facilitated sequentially through separate zones within a treatment train like the anaerobic, anoxic and aerobic process (A^2/O) [2], or by employing temporally sequentially phased

isolation ditches for creating anaerobic, anoxic and aerobic conditions such as Bio-Denipho process [3]. Recent scientific studies suggest, however, that simultaneous nitrification and denitrification (SND) may occur in certain treatment systems [3–6]. Dissolved oxygen (DO) gradients within microbial flocs may create two types of zones within each of these flocs, favourable for nitrifiers and denitrifiers respectively [7]. Heterotrophic nitrifiers and aerobic denitrifiers may also convert ammonia directly into gaseous nitrogen [6]. In the same time, the variation of oxygen concentration in corresponding zones creates mechanisms for phosphorus removal in such system by phosphorus accumulating organisms (PAOs) [8].

*Corresponding author.

In activated sludge processes, parameters such as hydraulic retention time (HRT), solid retention time (SRT), mixed liquor volatile suspended solids (MLVSS), organic loading (indicated by chemical oxygen demand (COD)), DO, temperature (T), and pH may all potentially influence the physical and biochemical aspects of the treatment processes [7–11]. However, DO plays a basic role in the controlling of these two processes [2].

In the phased isolation process, the parameters can be optimised by adjusting operation conditions much easily than other conventional activated sludge processes [3,8,9,11]. There is a periodic and alternative oscillation of organics and DO which is designed to create favourable zones or optimal mechanisms within a ditch [3,12]. The previous studies showed that the cycle length of the sequencing phases and ammonia set point are two important process control parameters [12]. Most of the previous studies focused mainly on the general treatment removal efficiencies through assessment of influent and effluent concentrations of COD, N and P [3,6,7,13]. However, information on the profiles of DO, COD, NH_4^+-N , NO_x-N , P showing the variation of operating variables in each phase within a complete operation cycle has been scarce [8]. In this study, we address this deficiency by presenting complete profiles of all these parameters through measurements; in the same time, an explanation on the variation of NH_4^+-N , NO_x-N and P has also been provided using the ASM2d [14] based on a unit flow concept.

2. Methods

2.1. The wastewater treatment plant (WWTP) and the Bio-Denipho system

The Beishiqiao wastewater treatment plant (WWTP) is located in Xi'an, China, with a capacity of $120,000 \text{ m}^3 \text{ d}^{-1}$. The WWTP consists of a grit and aerobic chamber (GAC), a Bio-Denipho process, and secondary settling tanks as shown in Fig. 1(a). The HRT

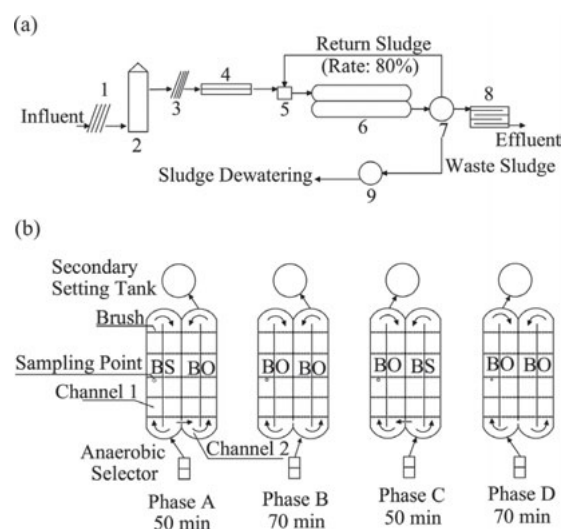


Fig. 1. (a) Simplified flow chart of Beishiqiao WWTP; the numbers denote: 1 – 25 mm screen; 2 – pumping station; 3 – 10 mm screen; 4 – grit and aerobic chamber; 5 – anaerobic selector; 6 – oxidation ditch; 7 – secondary setting tank; 8 – disinfection tank; 9 – sludge thickening tank. (b) Illustration of the four-phased Bio-Denipho process. Note: BO: Brushes in operation, BS: brushes on standby.

and SRT are 4.75 h and 18 d respectively, and MLSS of about $4200 \pm 200 \text{ mg l}^{-1}$. The typical wastewater quality is listed in Table 1.

The four-phased Bio-Denipho process is illustrated in Fig. 1(b). There is an “anaerobic selector” ($\text{DO} \leq 0.1 \text{ mg l}^{-1}$) prior to a two-channel ditch. The selector conventionally used for filamentous bacteria control [3], was also for promoting an environment for PAOs to accumulate excessive amounts of phosphorus in the Bio-Denipho system [8,15,16]. The system of ditches is a continuous flow, activated sludge system designed for biological nitrogen and phosphorus removal. The ditches are aerated by brush aerators and the mixed liquor in each channel is circulated by hydraulic propellers.

Table 1
Typical wastewater quality in Beishiqiao WWTP

	Influent after screen	Exit of grit and aerobic chamber	Anaerobic selector (filter)	Effluent of oxidation ditch (filter)	Effluent of secondary settling tank (filter)
COD (mg l^{-1})	624 (144)	360 (135)	94.40	27.20	25.80
TN (mg l^{-1})	49.21	44.78	24.04	6.62	4.98
NH_4^+-N (mg l^{-1})	43.61	38.74	17.50	1.47	1.19
NO_x-N (mg l^{-1})	1.40	2.54	3.43	3.22	2.42
$\text{PO}_4^{3-}-\text{P}$ (mg l^{-1})	4.64	3.80	9.63	0.23	0.39
TP (mg l^{-1})	8.03	4.08	9.91	0.34	0.60

The removal of nutrients is performed in phased isolation ditches with intermittent operations, in which brush aeration operation is so controlled that alternating zones for nitrification and denitrification and phosphorus releasing and accumulating within the two parallel channels are created through periodic variation of influent pathway and aeration state. The running time for phases A, B, C, and D are 50, 70, 50, and 70 min respectively, with a cycle of 240 min.

2.2. Analytical methods

Analyses of DO, COD, total nitrogen (TN), $\text{NH}_4^+\text{-N}$, $\text{NO}_x\text{-N}$, total phosphorus (TP), and orthophosphate ($\text{PO}_4^{3-}\text{-P}$) were carried out following the Standard Methods [17]. One fixed sampling point was selected in one channel of the ditch (Fig. 1(b)). Triplicate samples (3×1 l) were taken from the sampling point at 10 min intervals within a cycle of the operation. DO and T were measured in situ, and samples were filtered before analysis. SRT was 18 d. T was $25 \pm 1^\circ\text{C}$, with a pH of 7.8 ± 0.5 during the experimental period.

2.3. Model calculation

Variation of DO, COD, $\text{NH}_4^+\text{-N}$, $\text{NO}_x\text{-N}$, and P in an operation cycle in the ditch was conducted based on the ASM2d [14,18], in which the processes of oxygen consumption, carbon degradation, nitrification, denitrification, and phosphorus removal were calculated based on the proposed fundamental processes.

Characterization of wastewater and biomass were determined based on measurements and the previous studies [14–18]. Procedures for the fractionation of organic matters, N, P and conversion factors are listed in Table 2; the values and stoichiometric coefficient of the kinetic parameters follow the procedures of Henze et al. [14] for the best fit to the analytical data, specifically for the first two phases where evident treatment characteristics of anoxic and aeration were observed. Model calculations were made at 0.1 min time intervals in the simulation process.

To calculate the dynamic treatment process, a “unit flow” model was proposed in the channel by assuming a plug-flow, so that a dilution factor of the influent with respect to circulation around the channel at a cross-section in a unit volume can be calculated. According to the flow rate, the change of variables with time within the unit flow can be calculated based on the ASM2d. The unit flow approach, in principle, is similar to that of “tanks-in-series” [18], except that a flowing unit rather than series of reactors was considered. The circulation time around the channel was

10 min at the recirculation rate of 25:1. In the model simulation, values for the stoichiometric coefficients and stoichiometric parameters, as well as values for the kinetic parameters are directly taken from the recommended values of ASM2d [14] except for reduction factor for anoxic activity of PAOs (η_{NO_3}). In this study, a value of 0.2 for η_{NO_3} gives the best fit to the analytical data (see later).

The basic modelling approach is similar for all the four phases. A brief illustration for Phase A is presented in Fig. 2. Since the circulation time of flow in the channel is known ($T = 10$ min), the whole flow may be viewed as a unit flow around the channel at the average speed or as N series of unit flow at a small time interval ($\Delta t = 0.1$ min, thus $N = 100$). For each unit flow, we have

$$QC_{i,t} - QC_{i,t+\Delta t} = r_i Q \Delta t \quad (1), \text{ or}$$

$$C_{i,t} - C_{i,t+\Delta t} = r_i \Delta t \quad (2)$$

$$r_i = \sum_j v_{ij} \rho_j \quad (3) \text{ (see also Ref. [14])}$$

where the C_i is the concentration of component i in ASM2d, such as S_F , S_{NH_4} , X_s etc.; Q = the flow rate; r_i = reaction rate of the component i ; v_{ij} = the stoichiometric coefficients and ρ_j = the process rate. Note that when SO_2 (or DO) was calculated for a unit flow at the position of brush an extra amount of DO input was incorporated according to DO diffusion capacity of the brush into Eq. (1).

The values of initial concentrations of each components $C_{0,i}$ at $t = 0$ (starting point of a complete cycle of the four phases) were taken from the measurements at the cross section of entrance. The values of concentrations of each component $C_{\text{inf},i}$ at the cross section of entrance of influent (Fig. 2) at other times was calculated using Eq. (4):

$$Q_{\text{inf}} C_{\text{inf},i} + Q_c C_{c,i} = (Q_{\text{inf}} + Q_c) C_{\text{ent},i} \quad (4)$$

where Q_{inf} = influent flow rate to the ditch; $C_{\text{inf},i}$ = the concentration of component i of influent (to the ditch). Q_c = the circulation flow (Fig. 2) and $C_{c,i}$ = the concentration of component i in neighbouring flow unit in the upstream. $C_{\text{ent},i}$ = the concentration of component i at entrance cross section.

Table 2

Procedure for the fractionation of organic matter, nitrogen and phosphorus in wastewater, measured in this study. "Influent" was sampled at the outlet of the "Grit and aerobic Chamber". "Effluent" was sampled from outlet of secondary settling tank

Symbol	Name	Value	Unit	Symbol	Name	Value	Unit
Soluble components							
S_{O_2}	Dissolved oxygen	0	$g\ O_2\ m^{-3}$	$COD_{tot,inf}$	Influent total COD	360	$g\ COD\ m^{-3}$
S_F	Readily biodegradable substrate	79.2	$g\ COD\ m^{-3}$	$COD_{f,tot}$	Influent COD in filtered sample	135.2	$g\ COD\ m^{-3}$
S_A	Fermentation products (acetate)	32.4	$g\ COD\ m^{-3}$	$COD_{tot,eff}$	Effluent COD in filtered sample	25.2	$g\ COD\ m^{-3}$
S_{NH_4}	Ammonium	38.8	$g\ N\ m^{-3}$	$COD_{f,eff}$	Effluent COD	24.8	$g\ COD\ m^{-3}$
S_{NO_3}	Nitrate (plus nitrite)	2.6	$g\ N\ m^{-3}$	COD_{VFAs}	COD from VFAs	79.2	$g\ COD\ m^{-3}$
S_{PO_4}	Phosphate	3.8	$g\ P\ m^{-3}$				
S_I	Inert, non-biodegradable organics	23.6	$g\ COD\ m^{-3}$				
S_{ALK}	Bicarbonate alkalinity	5	mole $HCO_3^-\ m^{-3}$				
Particulate components							
X_I	Inert, non-biodegradable organics	23.6	$g\ COD\ m^{-3}$	$S_A = COD_{VFAs}$			
X_S	Slowly biodegradable substrate	156	$g\ COD\ m^{-3}$	$Ss = COD_{f,tot} - S_I$		$X_I = (1 - \alpha)\ COD_{susp,inf}$	
X_H	Heterotrophic biomass	32.1	$g\ COD\ m^{-3}$	$S_F = S_S - S_A$		$X_S = \alpha\ COD_{susp,inf}$	
X_{PAO}	PAO	0	$g\ COD\ m^{-3}$	$S_A = COD_{VFAs}$		$\alpha = [(BOD_{tot} - S_S)] / COD_{susp,inf}$	
X_{TP}	Stored poly-phosphate of PAO	0	$g\ P\ m^{-3}$	$S_I = 0.95\ COD_{f,eff}$		$BOD_{tot} = BOD_5 / (1 - e^{-5k})$	
X_{PHA}	Organic storage products of PAO	0	$g\ COD\ m^{-3}$	$Ss = COD_{f,tot} - S_I$		$COD_{susp,inf} = COD_{tot,inf} - COD_{filt,inf}$	
X_{AUT}	Autotrophic, nitrifying biomass	0	$g\ COD\ m^{-3}$	$S_A = COD_{VFAs}$			
X_{TSS}	Particulate material	211.7	$g\ TSS\ m^{-3}$	$S_I = 0.95\ COD_{f,eff}$			

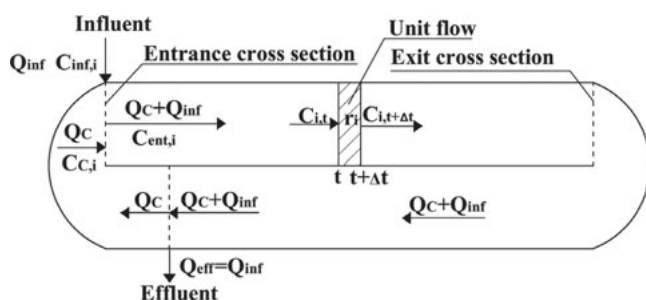


Fig. 2. An illustration of unit flow model for Phase A (see also Fig.1 (b)).

3. Results

3.1. DO

The measured profile of DO for each phase was presented in Fig. 3(a). The differences in DO profiles are resulted from the influent flow pattern, the brush operation state, and consumption rates of DO as well. In phase A, DO was low ($0.2\text{--}0.3\text{ mg l}^{-1}$), a typical anoxic condition. A small but immediate up-surge of DO from 0.3 to 0.5 mg l^{-1} was observed in phase B. This condition stayed for 40 min, then the DO increased gradually up to 3 mg l^{-1} . In phase C, DO was high ($2\text{--}3\text{ mg l}^{-1}$). In phase D, with the influent switched back to channel 1 with a controlled brush operation, DO first dropped to a low value, then gradually increased before turning down to a low value again. The simulation was carried out according to the actual operation status of brushes by assuming an aeration capacity of a brush to the best fit for the measured DO at corresponding points.

3.2. Dissolved COD

Results of COD measurements are presented in Fig. 3(b), a different feature is observed for each phase, although the magnitude of concentration variation is not so large. In phase A, there was a periodic variation of COD accompanying the mixed liquor hydraulic circulation in the channel (~ 10 min). In phase B, the COD constantly decreased. In phase C, there was a slight COD increase due to the resumption of inflow of influent in channel 2. In comparison, COD increased evidently at the beginning of phase D and then declined. In the ASM2d model simulation, dissolved organic matter (or dissolved COD) was composed of fermentation products (S_A), fermentable and readily biodegradable organic substrates (S_F), and inert organic matter (S_I).

3.3. NH_4^+-N

Fig. 3(c) presents a distinct measured profile of NH_4^+-N at each phase. The phase A was featured with a sharp

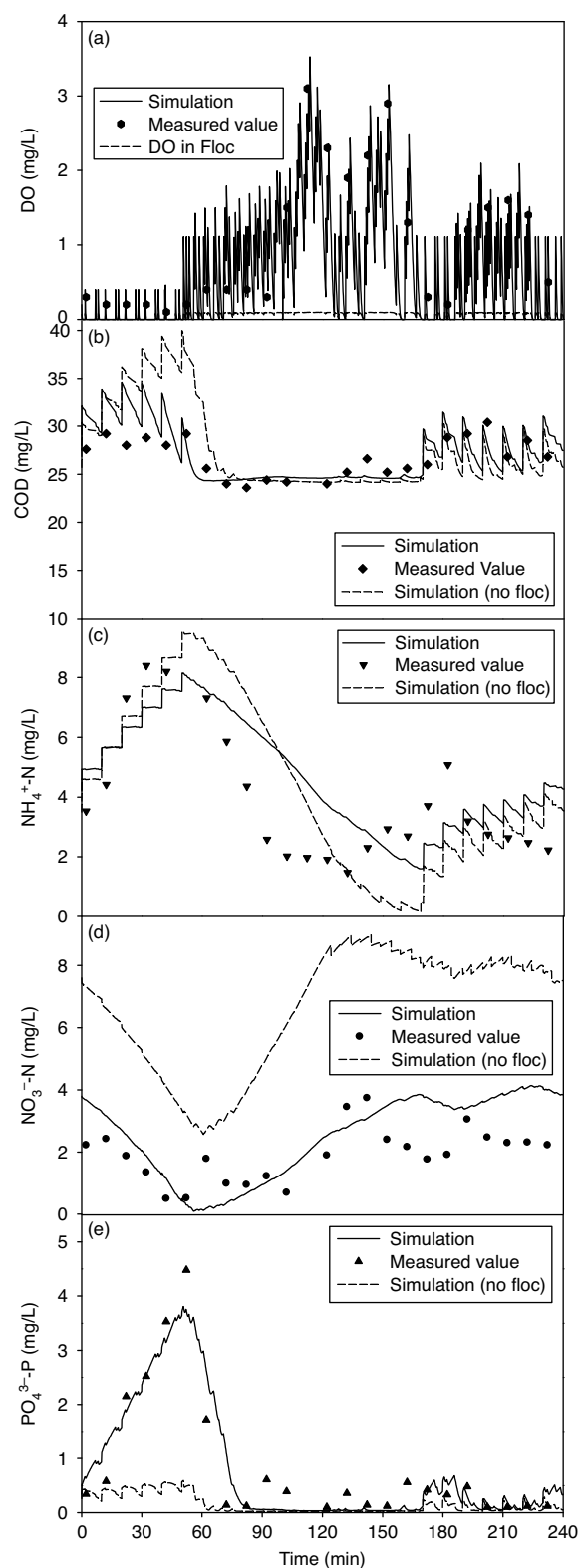


Fig. 3. Variables in the four-phased Bio-Denitro process as function of time. Solid legends: analytical data; solid lines: calculated values based on modified ASM2d; broken lines: calculated values based on the ASM2d. (a) DO; (b) dissolved COD; (c) NH_4^+-N ; (d) NO_3^--N ; (e) $\text{PO}_4^{3--}\text{P}$.

increase of $\text{NH}_4^+\text{-N}$. In phase B, however, the $\text{NH}_4^+\text{-N}$ plummeted to a very low level. It should be noticed that $\text{NH}_4^+\text{-N}$ was maintained at low concentrations across phases C and D, where the mixed liquor exited from the ditch for clarification.

3.4. $\text{NO}_x\text{-N}$

$\text{NO}_x\text{-N}$ versus time is presented in Fig. 3(d). Since the T was high, the $\text{NO}_x\text{-N}$ was largely in the form of nitrate, for little nitrite accumulation in the nitrification process [4]. In phase A, there was an evident continuous decrease of $\text{NO}_x\text{-N}$ to a low concentration. In contrast, the $\text{NO}_x\text{-N}$ in phase B gradually increased. Interestingly, the $\text{NO}_x\text{-N}$ in phases C and D, however, was relatively stable at low concentrations.

3.5. Phosphorus

In Fig. 3(e), a high rate of phosphorus release was observed in the phase A, with a higher rate of phosphorus uptake by biomass in phase B. It is likely that the fastest microbial phosphorus removal occurred within this short period, with only the slow rate of phosphorus release and uptake proceeding in phases C and D.

4. Discussions

From Fig. 3(a–e), the variables of DO, COD, $\text{NH}_4^+\text{-N}$, $\text{NO}_x\text{-N}$, $\text{PO}_4^{3-}\text{-P}$ exhibited distinctive profiles as function of reaction time within each phase. These features are the reflection of the consequences of the related biochemical reaction processes under each of the concrete conditions. A brief discussion based on the rates of the fundamental reaction processes for organics degradation, nitrification–denitrification, phosphorus removal in the ASM2d [12,18,19] would be beneficial to a better understanding of treatment mechanisms behind the data profiles.

Simulated values of COD, $\text{NH}_4^+\text{-N}$, $\text{NO}_x\text{-N}$, $\text{PO}_4^{3-}\text{-P}$ based on the ASM2d were presented in Fig. 3(b–e) (broken lines). A large deviation between the simulated values and the analytical data was seen for $\text{NO}_x\text{-N}$, $\text{PO}_4^{3-}\text{-P}$. This deviation is likely due to the oxygen gradients within biomass flocs, which is believed to be partially responsible for SND in some activated sludge processes [7]. Most likely there is a difference in oxygen contents within the biomass flocs and the bulk water of the mixed liquor. Here, we introduce a fraction coefficient (α) to differentiate the fraction of the organisms within the core of biomass flocs under lower oxygen contents from those outside the flocs or in bulk liquor (Fig. 4).

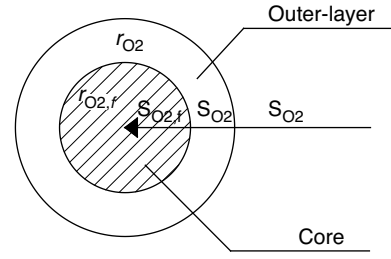


Fig. 4. Proposed configuration of biomass flocs.

The concentration of DO within the biomass flocs can be calculated by the equation below following the similar approach in the model:

$$S_{O_2,f} = S_{O_2} \left(\frac{k_{O_2}}{S_{O_2} + k_{O_2}} \right) \quad (5)$$

where $S_{O_2,f}$ = oxygen concentration within the biomass flocs; S_{O_2} = oxygen concentration in the bulk mixed liquor; k_{O_2} = dissolved oxygen diffusion limiting coefficient (=0.10). Therefore, for each process component, the total rate is:

$$r_T = \alpha \times r_{S_{O_2,f}} + (1 - \alpha) \times r_{S_{O_2}} \quad (6)$$

where r_T = total reaction rate for each component; $r_{S_{O_2,f}}$ = reaction rate of organisms within flocs; $r_{S_{O_2}}$ = reaction rate of organisms in bulk or outside the flocs.

With this modification of the ASM2d, it was found that, when α is at 0.68 a best fit can be obtained (Fig. 3(b–e), solid lines). Relevant average rates of reactions mechanisms for each phase were calculated and presented in Table 3.

4.1. Phase A

The phase A at low DO concentration ($0.2\text{--}0.3 \text{ mg l}^{-1}$) (Fig. 3(a)), is dominantly an anoxic “denitrification” and phosphorus releasing process. From Table 3, the largest organic carbon consumption or degradation comes from the two processes of denitrification with fermentable and readily biodegradable organic substrate (S_F), and the consumption of fermentation products (S_A) of cell internal storage of poly-hydroxy-alkanoates (PHA) by PAOs.

A higher rate of “de-nitrification” by the anoxic heterotrophic growth on S_F and S_A , and a low rate of conversion of ammonia to $\text{NO}_x\text{-N}$ by suppressed autotrophic growth under the condition (Table 3) lead to the reduction of $\text{NO}_x\text{-N}$. The increase of $\text{NH}_4^+\text{-N}$ was resulted from the combined effect of a low rate of ammonia degradation and accumulation of influent $\text{NH}_4^+\text{-N}$.

Table 3
Average reaction rates ($\text{g h}^{-1}\cdot\text{m}^{-3}$) of S_F , S_A , $\text{NO}_x\text{-N}$, $\text{NH}_4^+\text{-N}$ and $\text{PO}_4^{3-}\text{-P}$ in each of the four phases based on modified ASM2d

	S_F	S_A				S_{NH_4}				S_{NO_3}				S_{PO_4}			
		1	2	3	4	1	2	3	4	1	2	3	4	1	2	3	4
1	41.2	364.5	301.1	218.2		0.4	3.6	3.0	2.2								
2	402.0	178.1	230.6	305.9		4.0	1.8	2.3	3.1								
3	671	79.7	23.2	26.0		0.7	0.8	0.2	0.3								
4	-145.6	-412.2	-439.0	-648.4		-2.0	-5.7	-6.0	-8.9					-0.4	-1.0	-1.1	-1.6
5					-30.4	-48.1	-7.0	-95.1						-0.4	-0.6	-0.1	-1.2
6	-497.2	-178.6	-70.1	-169.1		-6.8	-2.5	-1.0	-2.3	-65.2	-23.4	-9.2	-22.2	-1.2	-0.4	-0.2	-0.4
7					-106.5	-45.5	-1.1	-24.7		-14.0	-6.0	-0.1	-3.2	-1.3	-0.6	0.0	-0.3
8	-255.5	-108.2	-37.7	-91.4	255.5	108.2	37.7	91.4	7.7					2.6	1.1	0.4	0.9
9									10.6					3.3	3.3	3.3	3.3
10					-379.2	-87.3	-32.5	-240.7						151.7	34.9	13.0	96.3
11														-38.1	-143.7	-61.5	-111.4
12										-9.3	-3.6	-2.5	-6.5	-133.1	-51.7	-35.1	-93.2
13						-1.2	-9.9	-8.0	-6.4					-0.4	-2.8	-2.3	-1.8
14						-4.4	-3.6	-4.4	-4.9	-13.1	-10.7	-13.2	-14.7	-1.2	-1.0	-1.3	-1.4
15						2.9	2.9	2.9	2.9					0.9	0.9	0.9	0.9
16														85.9	86.1	86.3	86.2
17					5.7	6.0	3.6	3.8									
18						-8.9	-89.6	-66.3	-53.0	8.8	88.1	65.2	52.1	0.0	-0.4	-0.3	-0.3
19						0.4	0.4	0.4	0.4					0.1	0.1	0.1	0.1
Tot	-388.0	-76.7	8.2	-358.8	-246.1	-66.7	0.7	-265.4	-2.7	-92.0	-65.5	-58.7	40.3	5.5	68.3	-75.9	2.1

Note: 1 – Aerobic hydrolysis; 2 – Anoxic hydrolysis; 3 – Anaerobic hydrolysis; $\text{X}_{\text{H}};$ (4 – Growth on S_A ; 5 – Growth on S_F ; 6 – Denitrification with S_A ; 8 – Fermentation of S_F ; 9 – Lysis; $\text{X}_{\text{PAO}};$ (10 – Storage of PHA; 11 – Aerobic storage of PP; 12 – Anoxic storage of PP; 13 – Aerobic growth; 14 – Anoxic growth; 15 – Lysis of PAO; 16 – Lysis of PP; 17 – Lysis of PHA; $\text{X}_{\text{AUT}};$ (18 – Aerobic growth; 19 – Lysis).

High rate release of phosphorus (S_{PO_4}) by PAOs from poly-phosphate (PP) and lysis of PP resulted in an accumulation of (S_{PO_4}). This observation agrees with previous study that phosphorus release occurs under anoxic condition with sufficient organic food supply [20]. In simulation, a value of 0.2 for η_{NO_3} of PAOs, instead of 0.6 (recommended by ASM2d), produced a best fit to the analytical data of NO_x-N , $PO_4^{3-}-P$. The ASM2d recommended value (0.6) would have overestimated the rate of uptake of $PO_4^{3-}-P$ by anoxic storage of PP in the Bio-Denipho treatment system. This may be due to very low oxygen concentrations close to zero, which lead to a suppressed anoxic storage of PP.

4.2. Phase B

In this phase, growth of heterotrophic organisms (X_H) on S_F accounted for most of the organics consumption (Table 3). This consumption rate is greater than that of aerobic and anoxic hydrolysis. In addition, due to no replenishment of organics from influent the organics contents (COD) declined. Furthermore, there was no organic overloading for the nitrification process under the condition.

The rapid reduction of NH_4^+-N in this phase is mainly due to aerobic growth of autotrophic organisms (X_{AUT}) (Table 3). Due to the same reason, concentration of NO_x-N increased in the mixed liquor. There was a low rate of denitrification by X_H and noticeable denitrification activities by PAOs. It was reported that clearly featured sequencing phases are important for nitrification and denitrification processes in a two stage treatment process [1,16]. However, the transition between the phases did not appear to create such a problem for nitrogen removal in the Bio-Denipho system.

In the same time, the S_{PO_4} decreased sharply in the mixed liquor. This is due to the rapid consumption of S_{PO_4} by aerobic cell internal storage of PP under the aerobic condition.

4.3. Phase C

In this phase, DO was relatively high. The mixed liquid from channel 2 carried over large amount of X_S but relatively small amount of S_F and S_A into the channel 1. The rates of aerobic and anoxic hydrolysis over-weighted slightly rate of heterotrophic organism growth on S_F resulting in a very small increase of COD.

Model simulation indicated that there was a moderate rate of autotrophic nitrification in this phase resulting in a decrease of NH_4^+-N . Denitrification here mainly relied on heterotrophic organisms denitrification with S_F and anoxic growth of PAOs. However, the total rate was much smaller than that of phase A.

In this phase, the reduction rate of S_{PO_4} was less than half of that in phase B by aerobic cell internal storage of PP; thus a small net increase rate of S_{PO_4} was observed.

4.4. Phase D

In this phase, high concentrations of organics, NH_4^+-N and $PO_4^{3-}-P$ from influent was again switched back to channel 1 and the operation of brushes maintained a relatively high DO concentration. From Table 3, the rates of COD degradation exceeded the rate of entrapped organics hydrolysis; however, because of the high input from the influent accumulation of S_F and S_A there was a slight increase of COD.

The reduction rate of NH_4^+-N was smaller than that of phase B and C due to a lower DO concentration in the mixed liquor and higher organics load in mixed liquor due to influent input. Compared with phase B and C, nitrification rate is smaller and denitrification rate is greater.

From the reaction mechanisms, due to the replenishment of phosphorus in the influent under the moderate aeration condition, phosphate release rate by PAOs was higher than phase C. The increased aerobic storage of X_{PP} lead to a higher rate of taking-up of S_{PO_4} . Thus, no accumulation of phosphorus was observed. In addition, from model calculation, it appeared that direct influent-flow into the channel in this phase provides a proper supply of organics for phosphorus uptake by PAOs. It has been suggested that biological phosphorus removal would be enhanced with the existence of sufficient organics [19–22].

Finally, we comment that the introduction of the fraction coefficient α for the best fit to the analytical data, especially for NO_x-N and $PO_4^{3-}-P$, indicates that anoxic denitrification and phosphorus releasing within the biomass flocs are important for the Bio-Denipho treatment system. It has been reported that up to 50% of NO_x-N was removed by SND under low DO and intermittent aeration conditions, and 15% under fully aerobic conditions, with concurrent oxygen and nitrite and nitrate utilization or denitrification occurring in anoxic microzones inside activated sludge flocs [6]. Fast and large variation of DO concentrations from low values in an intermittently-aerated cyclic activated-sludge single-reactor with a high concentration of MLSS may favour the SND [16].

5. Conclusions

Profiles of DO, COD, NH_4^+-N , NO_x-N , TP and $PO_4^{3-}-P$ versus time have been established through measurements for a four-phased Bio-Denipho process.

A simple hydraulic approach was proposed for analyses of the process base on the ASM2d model. Characteristic profiles of COD, NH_4^+-N , NO_x-N and $\text{PO}_4^{3-}-\text{P}$ at each phase was analysed based on the fundamental reaction mechanisms. Model simulation indicated that denitrification and phosphorus releasing within the biomass flocs are important for nitrogen removal and biological phosphorus removal in the treatment system.

Acknowledgements

This work was supported by the “Program for Changjiang Scholars and Innovative Research Team in University” (PCSIRT) (Grant No. IRT0853) and the Research Foundation of Xi’an University of Architecture and Technology (No. DB03069, DB03087). Thanks extend to Dr. Nirmala Dinesh at SA Water Corporation for her review of the text of this paper.

References

- [1] Metcalf & Eddy, T. Asano, F.L. Burton, H.L. Leverrenz, R. Tsuchihashi and G. Tchobanoglous, *Water Reuse: Issues, Technologies, and Applications*, McGraw-Hill Education (Aisa) Co and Tsing Hua University Press, 2008.
- [2] Metcalf & Eddy, G. Tchobanoglous and F.L. Burton, *Wastewater Engineering, Treatment, Disposal, and Reuse*, 3rd ed., McGraw-Hill, New York, 1991.
- [3] S. Isaacs, Automatic adjustment of cycle length and aeration time for improved nitrogen removal in an alternating activated sludge process, *Water Sci. Technol.*, 35 (1) (1997) 225–232.
- [4] X. Hao, H.J. Doddema and J.W. van Groenestijn, Conditions and mechanisms affecting simultaneous nitrification and denitrification in a Pasveer oxidation ditch, *Bioresour. Technol.*, 59 (1997) 207–215.
- [5] E.V. Münch, P. Lant and J. Keller, Simultaneous nitrification and de-nitrification in bench-scale sequencing batch reactors, *Water Res.*, 30 (1996) 277–284.
- [6] H.W. Zhao, D.S. Mavinic, W.K. Oldham and F.A. Koch, Controlling factors for simultaneous nitrification and de-nitrification in a two-stage intermittent aeration process treating domestic sewage, *Water Res.*, 33 (4) (1999) 961–970.
- [7] K.H. Hong, D. Chang, S.W. Kang, J.M. Hur, S.B. Han and Y. Sunwoo, Effect of cycle length and phase fraction on biological nutrients removal in temporal and spatial phase separated process, *J. Ind. Eng. Chem.*, 14 (2008) 520–525.
- [8] E. Bundgaard, K.L. Andersen and G. Petersen, BIO-DENITRO and BIO-DENIPHO Systems—experiences and advanced model development: the Danish systems for biological N and P removal, *Water Sci. Technol.*, 21 (1989) 1727–1730.
- [9] J. Makinia, K.H. Rosenwinkel and V. Spering, Long term simulation of the activated sludge process at the Hanover-Gummershals pilot WWTP, *Water Res.*, 39 (2005) 1489–1502.
- [10] T.G. Potter, B. Koopman and S.A. Svoronos, Optimization of a periodic biological process for nitrogen removal from wastewater, *Water Res.*, 30 (1996) 142–152.
- [11] H. Zhao, H. Isaacs, H. Sørensen and M. Kümmel, A novel control strategy for improved nitrogen removal in an alternating activated sludge process —Part II. Control development, *Water Res.*, 29 (1995) 535–544.
- [12] H. Zhao, H. Isaacs, H. Sørensen and M. Kümmel, A novel control strategy for improved nitrogen removal in an alternating activated sludge process —Part I. Process analysis, *Water Res.*, 28 (1994) 521–534.
- [13] S. C. F. Meijer, M. C. M. Van Loosdrecht and J. J. Heijnen, Metabolic modelling of full-scale biological nitrogen and phosphorus removing wwtp’s, *Water Res.*, 35(2001)2711–2723.
- [14] M. Henze, W. Gujer, T. Mino and M.v. Loosdrecht, *Activated Sludge Models ASM1, ASM2, ASM2d AND ASM3*, IWA Publishing in its Scientific and Technical Report series, London, UK, 2000.
- [15] D. Brdjanovic, M.C.M. van Loosdrecht, P. Versteeg, C.M. Hooijmans, G.J. Alaerts and J.J. Heijnen, Modeling COD, N and P removal in a full-scale WWTP Haarlem Waarderpolder, *Water Res.*, 34 (3) (2000) 846–858.
- [16] Y. Hyungseok, H.A. Kyu, J.L. Hyung, H.L. Kwang, J.K. Youn and G.S. Kyong, Nitrogen removal from synthetic wastewater by simultaneous nitrification and denitrification (SND) via nitrite in an intermittently-aerated reactor, *Water Res.*, 33 (1) (1999) 145–154.
- [17] *Standard Methods for the Examination of Water and Wastewater*, 19th ed., American Public Health Association/American Water Works Association/Water Environment Federation, Washington, DC, USA, 1996.
- [18] B. Petersen, K. Gernaey, M. Henze and P.A. Vanroieghem, Evaluation of an ASM1 model calibration procedure on a municipal-industrial wastewater treatment plant, *J. Hydroinform.*, 4 (1) (2002) 15–38.
- [19] G.A. Ekama, G.v.R. Marais and I.P. Siedritz, *Theory, design and operation of nutrient removal activated sludge process*, Water Research Commission, University of Cape Town, Pretoria, South Africa, 1984.
- [20] J. Meinhold, H. Pedersen, E. Arnold, S. Issacs and M. Henze, Effect of continuous addition of an organic substrate to the anoxic phase on biological phosphorus removal, *Water Sci. Technol.*, 38 (1) (1998) 97–105.
- [21] H. Temmink, B. Petersen, S. Isaacs and M. Henze, Recovery of biological phosphorus removal after periods of low organic loading, *Water Sci. Technol.*, 34 (1–2) (1996) 1–8.
- [22] U. Sarkar, D. Dasgupta, T. Bhattacharya, S. Pal and T. Chakroborty, Dynamic simulation of activated sludge based wastewater treatment processes: case studies with Titagarh Sewage Treatment Plant, India, *Desalination*, 252 (2010) 120–126.